Journal of Macromolecular Science, Part A
Publication details, including instructions for authors and subscription information:
http://www.informaworld.com/smpp/title~content=t713597274

Smart pH-sensitive Alternating Copolymers of (Methylacrylamide-Hydroxyethylmethacrylate); Kinetic and Physical Properties

Mohammad M. Fares[a]; Ali A. Othman[a]
[a] Department of Applied Chemistry, Jordan University of Science & Technology, Irbid, Jordan

Online publication date: 01 December 2009

To cite this Article Fares, Mohammad M. and Othman, Ali A.(2010) 'Smart pH-sensitive Alternating Copolymers of (Methylacrylamide-Hydroxyethylmethacrylate); Kinetic and Physical Properties', Journal of Macromolecular Science, Part A, 47: 1, 61 — 70
To link to this Article: DOI: 10.1080/10601320903399750
URL: http://dx.doi.org/10.1080/10601320903399750

Journal of Macromolecular Science®, Part A: Pure and Applied Chemistry (2010) **47**, 61–70

ISSN: 1060-1325 print / 1520-5738 online
DOI: 10.1080/10601320903399750

Taylor & Francis
Taylor & Francis Group

Smart pH-sensitive Alternating Copolymers of (Methylacrylamide-Hydroxyethylmethacrylate); Kinetic and Physical Properties

MOHAMMAD M. FARES* and ALI A. OTHMAN

Department of Applied Chemistry, Jordan University of Science & Technology, P.O. Box 3030, 22110, Irbid, Jordan

Received February 2009, Accepted July 2009

The synthesis and physical properties of smart pH-sensitive (Methacrylamide-*alt*-2-hydroxyethylmethacrylate) copolymers (*i.e.* MAAm-*alt*-HEMA) were studied. The pH smart behavior determined using the cloud point technique showed a linear increase with increasing molar feed ratios of the copolymer. The rate of copolymerizations (R_p) determined by conventional %conv. vs. time method, and their apparent activation energies (E_a) were calculated. The reactivity ratios determined by Kelen-Tudos and Fineman-Ross techniques showed that the copolymer formed is an alternating type copolymer (*i.e.* $M_1M_2M_1M_2\ldots$). Furthermore, the calculated molar ratios ($\boldsymbol{F}_1$) and the experimental molar ratios determined using ^{13}C-NMR and FTIR were in very good agreement. The linear relationship of $ln\ (r_1r_2)$ vs. reciprocal of the temperature ($1/T$) shown in Equation 2 demonstrated an activation energy difference (*i.e.*, $(E_{12} + E_{21}) - (E_{11} + E_{22})$) and were found to be –118.4 kJ/mol confirming the alternating sequence behavior of MAAm and HEMA repeating units. The copolymers were characterized using ^{1}H-NMR, ^{13}C-NMR, FTIR, UV-Vis, TGA, DSC, powder X-ray, and SEM techniques.

Keywords: Smart, pH-sensitive, apparent activation energies, reactivity ratios values

1 Introduction

Stimuli-responsive polymers such as thermosensitive polymers (1, 2) and pH-sensitive polymers (3–5) play the most crucial role in the formation of hydrogels that can be successfully used in the control process of drug delivery. The change in pH values implies different acidic environment in the GI tract. This pH change encourages the formation of hydrogels that can only swell at certain pH value, and consequently, release periodically the contained drug at that pH. The increasing interest in site specific targeting, through oral administration, was due to its capability to cure well-known colon problems (6). The outstanding interest in controlled drug delivery system capable of delivering drug, using a pre-determined rate and time, implies many applications in pharmaceutical drug industries (7–9). The ultimate goal of this control process is to deliver proper concentration of the drug at proper time and/or site (10).

Polyelectrolyte polymers contain active pendant groups that can act differently at different pH, for example, if pendant group is COOH, then in basic medium it becomes COO^-, whereas it retains its structure in acidic medium. Furthermore, the NH_2 group is converted into NH_3^+ in acidic medium, whereas it retains its structure in basic medium. The degree of swelling and pH-responsiveness of these polymers depends on the number and structure of pendant groups, degree of acidity (*i.e.* pH) and structure of crosslinkers. Furthermore, the presence of charged molecules on the pendant groups stimulate electrostatic repulsion between similar charged molecules and hence, enhance probability of swelling and hydrophilic state. This hydrophilic state of polymer chains can be transformed into hydrophobic state if charges on molecules on pendant groups are neutralized through pH change (*i.e.* NH_3^+ transforms to NH_2), which lead to chain agglomeration and eventually lead to precipitation.

The excellent biocompatibility, stimuli-responsive behavior and physicochemical properties of poly(HEMA), in addition to its hydrolytic stability and its similarity to living tissues (11, 12), together with pH sensitive behavior of MAAm (13), have nominated them to be used in our work. Different molar feed ratios of MAAm to HEMA monomers that have different hydrophobic content and thus change in pH response were studied. The optimization

*Address correspondence to: Mohammad M. Fares, Department of Applied Chemistry, Jordan University of Science & Technology, P.O. Box 3030, 22110, Irbid, Jordan; E-mail: fares@just.edu.jo

of kinetic and physical properties of the formed (MAAm-*alt*-HEMA) copolymers such as rate of copolymerization (R_p) together with its apparent activation energies (E_a). Furthermore, reactivity ratios were determined using Kelen-Tudos (14), and Fineman-Ross techniques (15).

2 Experimental

2.1 Materials

Methacrylamide (MAAm) (Fluka Chemicals Co.) and 2-hydroxyethyl methacrylate (HEMA), 96% (Acros Chemical Co.) monomers were kept in a refrigerator and were used as received, *N,N,N′,N′*-Tetraethylenediamine (TEMED) (Sigma-Aldrich) used as an accelerator, was used as received, Potassium peroxodisulfate (KPS) (BDH Chemicals Ltd.), as an initiator, was further purified by recrystallization. All solvents and other chemicals were of analytical grade.

2.2 Preparation of (MAAm-*alt*-HEMA) Copolymers

Different molar ratios of MAAm to HEMA (*i.e.* M_{MAAm}/M_{HEMA}) equal to 0.66, 1.0, 1.3, 1.5, 3.0, and 9.0 were synthesized as follows; each monomer concentration were dissolved in 25 ml of de-ionized water, the solutions were sparged with N_2 for 5 min or until the monomer was dissolved. To each solution 5 ml of 10% (wt/wt) KPS and 5 ml of 10% (wt/wt) TEMED, with respect to total monomers weights, were added under N_2atmosphere. Then, the mixture was set in 250 ml round bottom flask and sealed under N_2 atmosphere for 3.5 h in a water-bath fixed at 30°C. After the copolymerization was complete, the product was poured in an excess amount of chloroform, stirred for 15 min, and washed with hot de-ionized water to remove homopolymers, then filtered and dried in an oven at 80 °C for 8–12 h. The samples were further purified via centrifugation. The weight average molecular weight was determined using a light scattering technique (16).

2.3 Phase Transition Determination

2.3.1. *Cloud point measurements*

A Shimadzu (JAPAN) UV-2401 spectrophotometer supplied with a heating control device were used to detect the cloud point at λ_{max} equals 289 nm. Each sample was exposed to a change in pH from 1 to 13 values and the percent transmittance (%T) was monitored at room temperature. The sudden % transmittance decay indicates the turbidity formation, which is a pre-step before precipitation. The cloud point was taken as the mid-point between the onset and end set of the %transmittance decay. All measurements were reproducible.

2.4 Instrumentation

^{1}H- and ^{13}C-NMR Spectroscopy: The ^{1}H- and ^{13}C-NMR spectra of the copolymers were recorded on a Bruker Biospin Spectrometer of 400 MHz in deuterated water and acetone; the samples were macerated in solvent for 1 day. Chemical shifts (δ) are given in ppm with tetramethylsilane (TMS) as an internal standard.

FT-IR Spectroscopy: FT-IR spectra were recorded via Thermo Nicolet (avator-360, USA) FT-IR spectrophotometer in the range of 4000−400 cm^{-1}using KBr pellets, The disks were prepared using a 6% (wt/wt) samples/KBr powders ratio.

TGA and DSC Thermal Analysis: All samples were studied using a Shimadzu TA-50 (Japan) thermogravimetric analysis (TGA) and DSC analyzer. The $T_{decomposition}$ measurements by TGA were carried out in aluminum pans containing 10 ± 0.5 mg samples under N_2 atmosphere at a heating rate of 10°C/min from a 25−500°C range. The glass transition temperature (T_g) was measured by first heating at 50°C/min, then cooling and then second heating rate at 2°C/min, the T_g was taken as the mid-point of transition.

X-ray Diffraction: The diffraction studies were performed using a Philips-Holland diffractometer (model PW 1729) equipped with copper as target material under the operational conditions of 30 KV, 40 mA and wavelength between 1.54060 Å. The samples were scanned between 5° and 100°.

Scanning Electron Microscope (SEM): The SEM was taken using Polaroid film; the samples in the form of films were mounted on the specimen stabs and coated with gold ion by sputtering method with (DSM 950 (ZEISS) model) (USA), Polaron (E6100) model. Electronic absorption spectroscopy was obtained on UNICAN (Helios Alpha).

3 Results and Discussion

3.1 Characterization of (MAAm-*alt*-HEMA) Copolymers

3.1.1. *^{1}H-, ^{13}C-NMR, and FTIR Spectroscopy*

Figures 1 and 2 show the ^{1}H-NMR and ^{13}C-NMR spectra of (MAAm-*alt*-HEMA) copolymer.

Figures 1 and 2 demonstrate the feature ^{1}H-NMR and ^{13}C-NMR spectroscopy for (MAAm-*alt*-HEMA) copolymer.^{1}H-NMR spectrum showed different peaks for MAAm moiety, a peak of C***H***$_3$ at $\delta = 0.99$ ppm; C***H***$_2$ (main chain) band at $\delta = 2.04$ ppm, and N***H*** at $\delta = 7.79$ ppm, whereas for HEMA moiety C***H***$_3$peak at $\delta = 1.14$ ppm; -O-C***H***$_2$peak at $\delta = 4.16$ ppm; −C***H***$_2$OH peak at $\delta = 3.89$ ppm; C***H***$_2$(main chain) peak at $\delta = 2.04$ ppm and O***H*** peak at $\delta = 4.88$ ppm.

^{13}C-NMR spectra showed signals of ***C***H$_3$ at $\delta =$ 18.78 ppm; ***C***H$_2$ (main chain) band at $\delta = 47.02$ ppm, ***C***=O signal at $\delta = 180.79$ ppm, ***quaternary C*** signal at

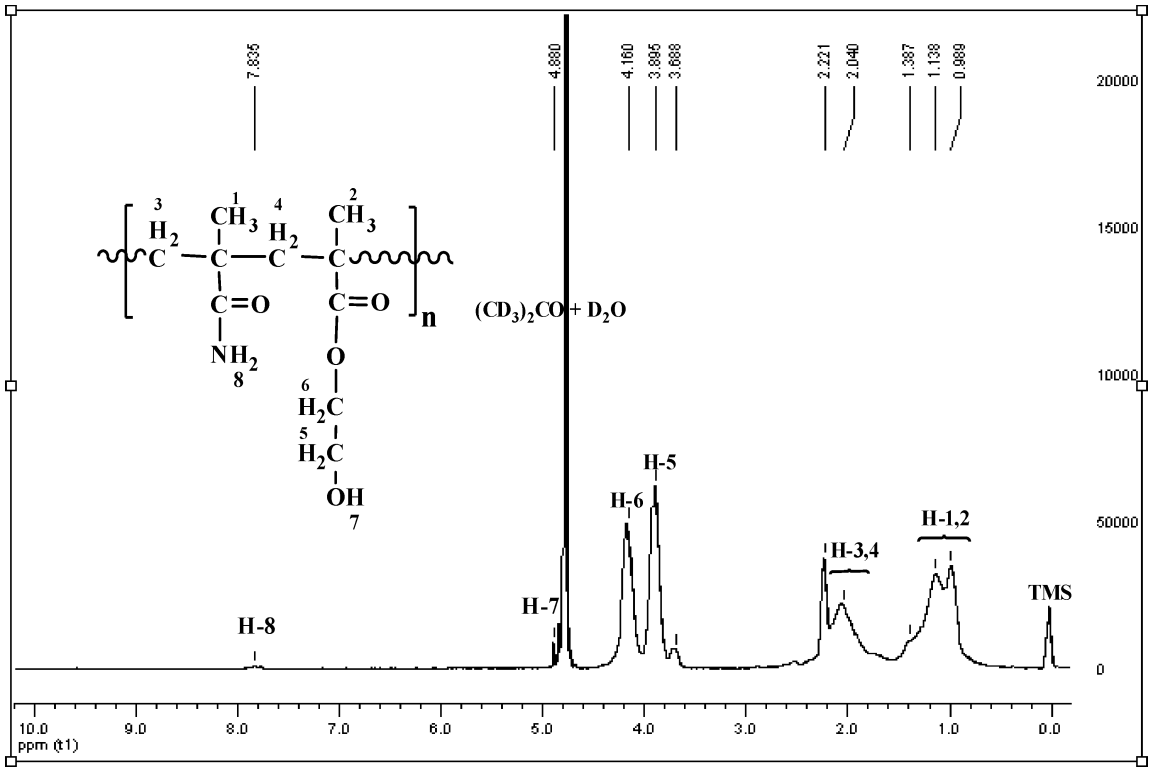

Fig. 1. ^{1}H-NMR spectrum of molar feed ratio = 0.66 of (MAAm-*alt*-HEMA) copolymer.

$\delta = 56.09$ ppm. For HEMA moiety, ***C***H_3 peak at $\delta = 20.73$ ppm; $-$O$-$***C***H_2peak at $\delta = 69.25$ ppm; $-$***C***H_2OH peak at $\delta = 61.48$ ppm; ***C***H_2(main chain) peak at $\delta = 64.95$ ppm; ***quaternary C*** signal at $\delta = 56.09$ ppm; and ***C***=O signal at $\delta = 181.70$ ppm. This confirms the formation of (MAAm-*alt*-HEMA) copolymer. The molar ratio of MAAm to HEMA in the copolymer were determined from the ratio C-9 (*i.e.* carbon of amide group in MAAm)

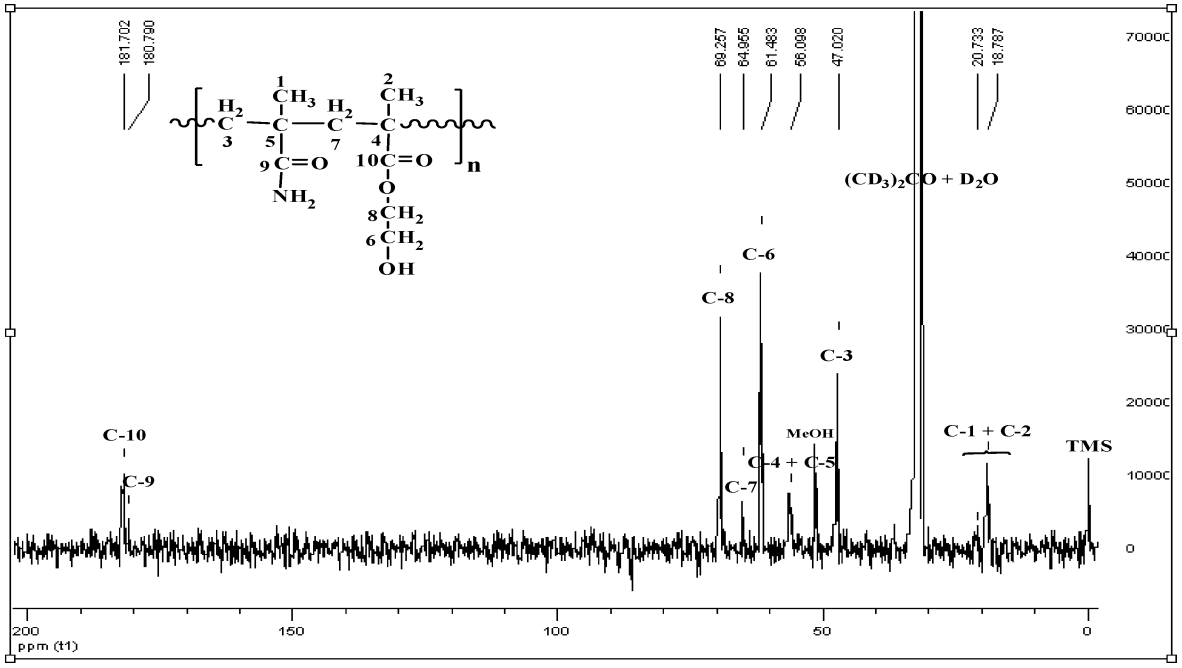

Fig. 2. ^{13}C-NMR spectrum of molar feed ratio = 1.0 of (MAAm-*alt*-HEMA) copolymer.

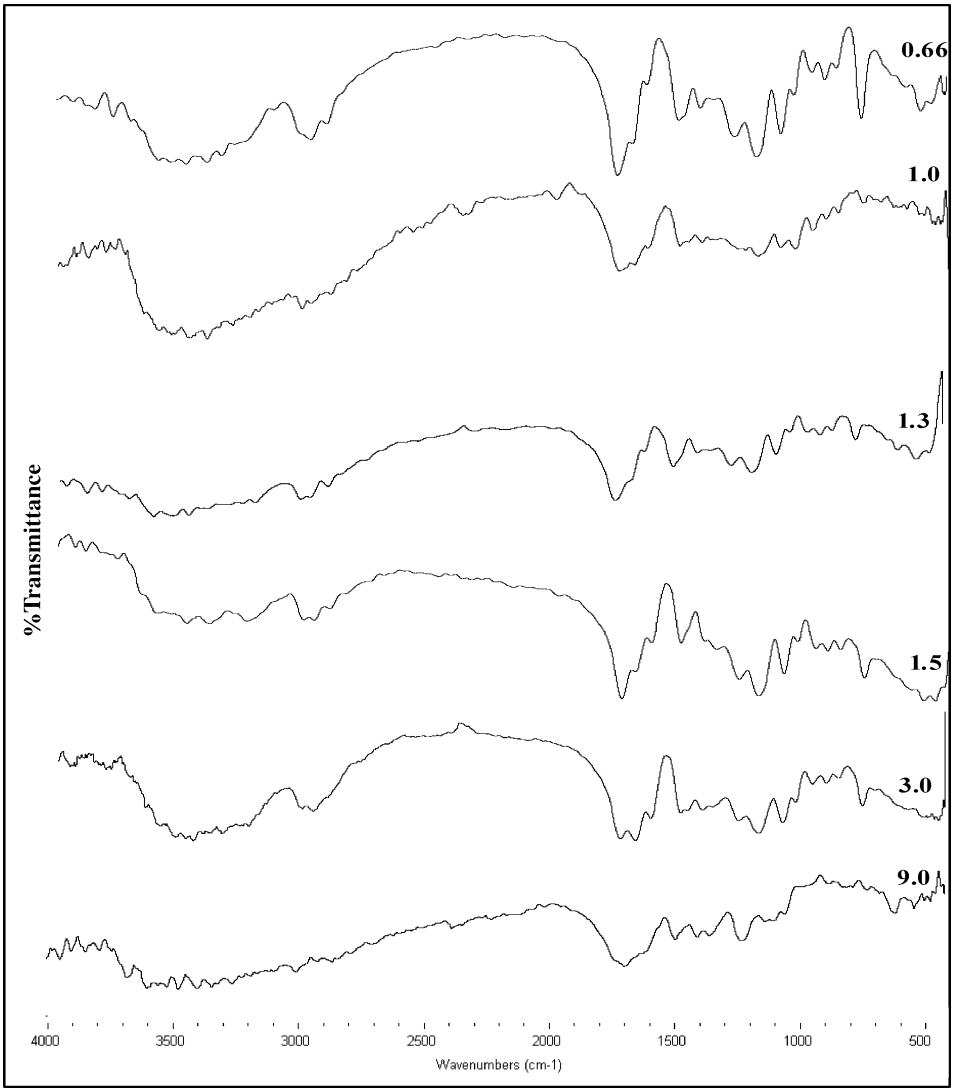

Fig. 3. FTIR spectra of all molar ratios of (MAAm-*alt*-HEMA) copolymer.

to C-10 (*i.e.* carbon of ester group in HEMA), which then will be used in Kelen-Tudos (14) and Fineman-Ross (15) techniques to determine the reactivity ratios of the copolymers. Furthermore, the molar ratio of the MAAm to HEMA in the copolymer were further deduced from FTIR spectra (Fig. 3) by determining the ratio of the absorbance of the carbonyl stretching of MAAm amide group located at 1666 cm^{-1} to the absorbance of the carbonyl stretching of HEMA ester group located at 1728 cm^{-1}. Furthermore, the OH stretching intensity at ~3500 cm^{-1} were decreased as molar feed ratio increased, which were expected due to lower HEMA content in the copolymer. However, as the molar feed ratio increased from 0.66 to 9.0, there were no systematic increases in the absorbance of carbonyl group of the amide, other than that of the ester group, which reflects a kind of alternation behavior of MAAm to HEMA groups. This will be further confirmed in the reactivity ratios section (see Reactivity ratio).

3.2 Thermal Analysis and X-Ray Diffraction

Figure 4 illustrates the TGA profile and its derivative for molar feed ratio = 1.0 of (MAAm-*alt*-HEMA) copolymer, which is an example for all the sample copolymers. Furthermore, Table 1 below shows the thermal properties determined for each molar feed ratio.

Two stages of decomposition temperatures appeared for (MAAm-*alt*-HEMA) copolymer, whereas it was single stage for homopolymers of MAAm and HEMA that clearly appeared from derivatives. The large increase of decomposition temperature of MAAm content in the copolymer with 30°C and that of HEMA content with 80°C in comparison to their homopolymers decomposition temperatures, reflectgreater consistency and rigidity of copolymer which were confirmed by T_g values. However; the large decrease in %crystallinity suggest that many H-bonding interactions between poly(MAAm) and poly(HEMA) chains were destroyed as a result of copolymerization process, which

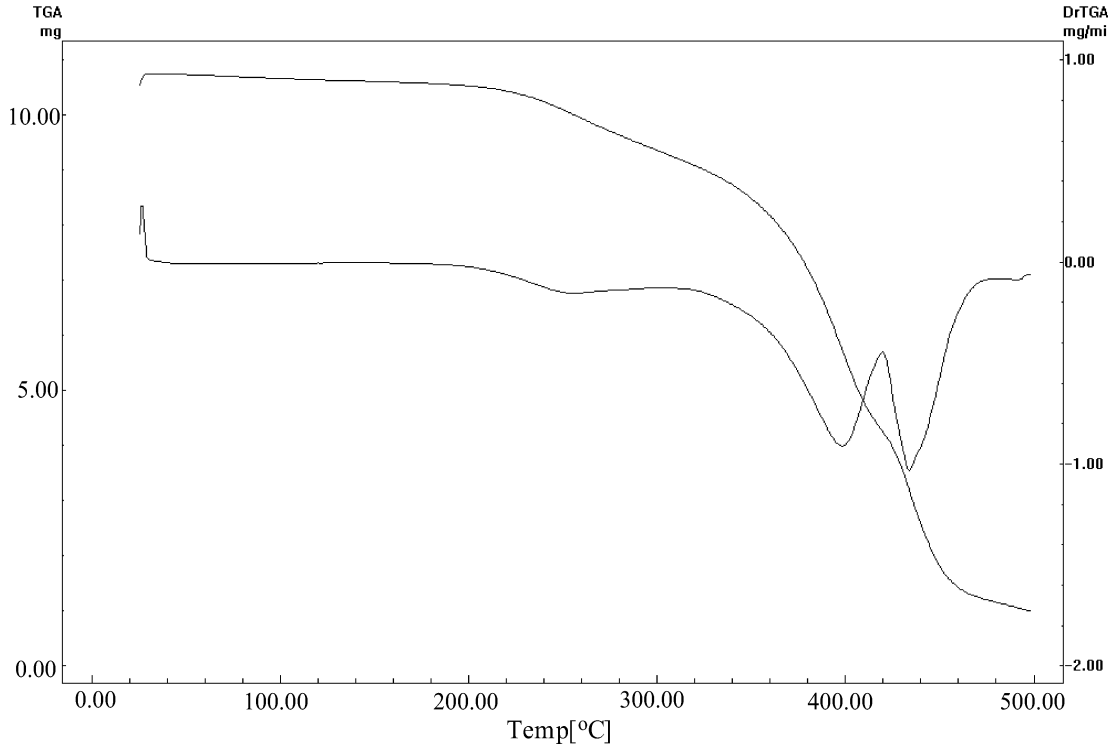

Fig. 4. TGA thermogram of molar feed ratio = 1.0 of (MAAm-*alt*-HEMA) copolymer.

eventually causes a decrease in %crystallinity values. This were shown by calculating the outermost peak (*i.e.*d_o-*spacings*).

Figure 5 shows the XRD patterns of poly(HEMA) and poly(MAAm) together with the different molar feed ratios of the (MAAm-*alt*-HEMA) copolymers. It is known that the location of outermost peak (d_o *spacing*) (higher scattering angle) is due to an intramolecular average distance along the backbone, whereas the innermost peak (d_i *spacing*) is strongly dependent on the length of the lateral groups and can be associated with intermolecular distance (17). Using Bragg's equation ($n\lambda = 2d\sin\theta$), the outermost peaks (d_o *spacing*) located at $2\theta = 33^\circ$ in poly(HEMA) and at $2\theta = 38^\circ$ in poly(MAAm) were found to be 2.7 and 2.4 Å, respectively. These *d-spacings* were almost very close to the H-bonding distance between polymer chains. Thus, the disappearance of these outermost peaks in the different molar feed ratios of the (*MAAm-alt-HEMA*) copolymers were in accordance with %crystallinity values.

The glass transition temperature (T_g) values emphasize the weakening of the intra and intermolecular forces between chains as a result of copolymerization process, which was in accordance with XRD pattern results. These inter- and intermolecular chain weakenings were also observed through T_g decrease values at elevated molar feed ratio increases from 0.66 to 1.3. Above 1.3 value, T_g value started

Table 1. The thermal properties of different molar ratios of (MAAm-*alt*-HEMA) copolymer

Sample	$T_{decomposition}(MAAm)(^\circ C)^\alpha$	$T_{decomposition}(HEMA)(^\circ C)^\alpha$	$T_g(^\circ C)^\beta$	$\%Crystallinity^\gamma$
poly(MAAm)	411	—	140	21.16
poly(HEMA)	—	318	104	11.1
0.66	430	386	92	4.4
1.0	434	399	88	3.6
1.3	438	398	92	—
1.5	444	395	118	—
3.0	436	392	122	2.0
9.0	404	370	134	—

$^\alpha$Derived from the derivative of thermogravimetric analyzer (DrTGA).
$^\beta$Derived from Differential Scanning Calorimeter (DSC).
$^\gamma$Derived from XRD pattern.

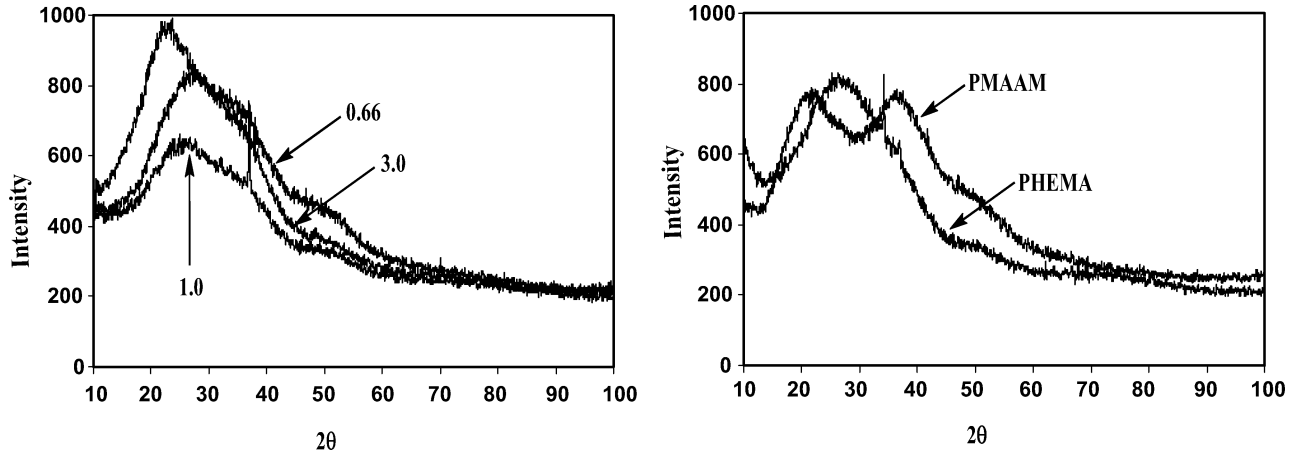

Fig. 5. XRD patterns of different molar ratios of (MAAm-*alt*-HEMA) copolymers.

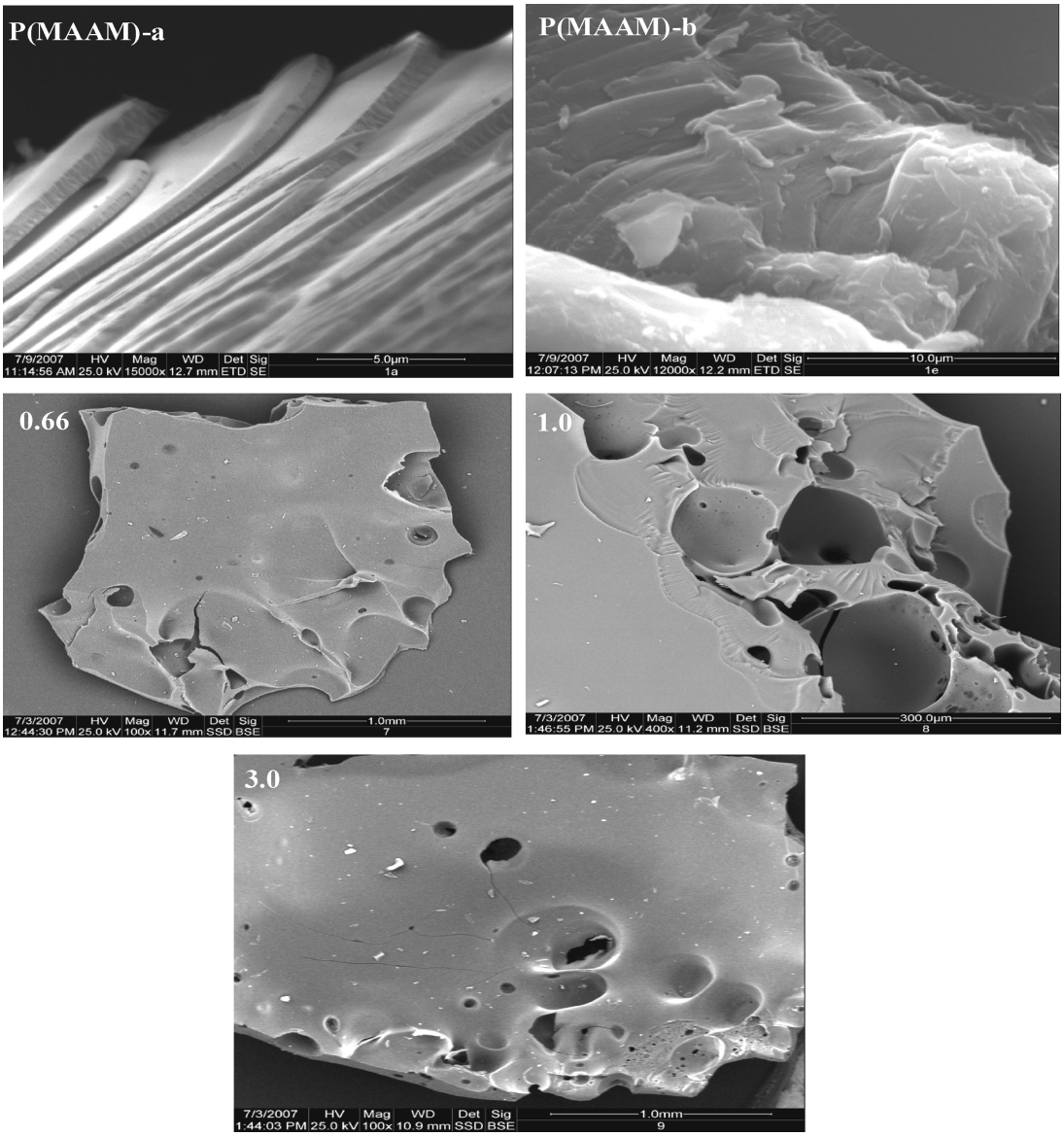

Fig. 6. The SEM micrographs of different molar ratios of (MAAm-*alt*-HEMA) copolymer together with poly(MAAm).

to incline due to the formation of more H-bonded chains until it reaches T_g =134°C for molar feed ratio = 9.0, which is relatively close to the pure poly(MAAm) (*i.e.* T_g =140°C).

3.3 Scanning Electron Microscope (SEM)

The morphology of poly(MAAm) and different molar ratios of the copolymers were shown in Figure 6. It could be clearly seen that poly(MAAm) formed two-dimensional layers which accumulated above each other. This accumulation of layers owed to the presence of strong H-bonding that aligns the chain above each other and consequently, larger %crystallinity was obtained. The relatively large crystallinity in poly(MAAm) and poly(HEMA) have almost disappeared in all the samples of the (MAAm-*alt*-HEMA) copolymers. This disappearance of crystallinity could be explained on the basis that the formed copolymer structure was of an alternating type (*i.e.* $M_1M_2M_1M_2\ldots$), which as a result led to lowering the amount of the H-bonding interactions , lowering %crystallinity and eventually forming a flat slippery rigid amorphous structures as Figure 6 suggests.

3.4 Kinetic Analysis

Table 2 summarizes the kinetic parameters for different molar feed ratios together with weight average molecular weight.

It could be clearly seen that an increase in molar feed ratio (*i.e.* increase in MAAm content in the copolymer) results in a drastic lowering in activation energy values. This lowering in activation energy was explained on the basis that the relative reactivity of MAAm monomer

Table 2. Kinetic parameters of different molar ratios of (MAAm-*alt*-HEMA) copolymer

Molar Ratio	*Temp. (°C)*	*Time (min.)*	*Yield (%)*	R_p *(g/L. sec.)*	E_a *(kJ/mol)*	M_w^a
0.66	5	15	0.67	0.0100	111.70	
		30	2.04			
		45	2.68			
		60	2.07			
	10	15	1.33	0.0230		1,000,000
		30	2.59			
		45	6.59			
		60	—			
	20	15	24.26	0.1192		
		30	26.29			
		45	34.92			
		60	26.48			
1.0	5	15	9.18	0.1822	30.17	
		30	20.48			
		45	31.68			
		60	25.02			
	10	15	—	0.0064		500,000
		30	0.23			
		45	0.78			
		60	1.57			
	20	15	25.73	0.1868		
		30	40.27			
		45	40.44			
		60	47.18			
3.0	5	15	2.31	0.0435	44.96	
		30	4.02			
		45	4.76			
		60	11.69			
	10	15	0.14	0.0097		1,250,000
		30	0.55			
		45	0.69			
		60	1.45			
	20	15	3.68	0.0847		
		30	6.61			
		45	9.39			
		60	8.05			

[a] Weight average molecular weight (M_w) determined from light scattering technique.

Table 3. Kinetic properties of (MAAm-*alt*-HEMA) copolymer

Kelen-Tudos						*Fineman-Ross*				
f_1^a	F_1^b *(exp.)*	F_1^c *(calc.)*	r_1	r_2	r_1r_2	F_1^b *(exp.)*	F_1^c *(calc.)*	r_1	r_2	r_1r_2
			0.0074	0.0514	0.0004			0.0180	0.1284	0.0023
0.66	0.487	0.483				0.444	0.459			
1.0	0.488	0.489				0.472	0.474			
1.3	0.489	0.492				0.473	0.482			
1.5	0.487	0.494				0.469	0.486			
3.0	0.477	0.499				0.475	0.503			
9.0	0.478	0.515				0.476	0.534			

[a]The molar feed ratio.
[b]The molar ratio in the copolymer as determined from ^{13}C-NMR and FTIR spectroscopy
[c]The calculated molar ratio as calculated from relation (1).

toward a radical chain was better than HEMA monomer, as deduced from their Q values in $Q-e$ scheme values and the Alfrey-Price equation (18). The Q value for MAAm was equal to 2.24, whereas the Q value for HEMA was equal to 1.78. Thus, the entrance rate of MAAm monomers into the growing chain was faster than HEMA monomers. No significant conclusions could be deduced from molecular weight determinations.

3.5 Reactivity Ratios

Two techniques were used to ensure exact determination of the reactivity ratios of the formed (MAAm-*alt*-HEMA) copolymer, namely Kelen-Tudos (14), and Fineman-Ross (15) techniques.

The molar ratio in the copolymer was determined using ^{13}C-NMR through the intensity ratio of C-9 (designated as monomer 1) to C-10 (designated as monomer 2) (Fig. 1). In addition, the molar ratio in the copolymer could be determined using FTIR spectroscopy through a ratio of the absorbance of carbonyl of amide group in MAAm (designated as monomer 1) at 1666 cm^{-1} to the absorbance of the carbonyl of ester group in HEMA (designated as monomer 2) at 1728 cm^{-1}. For more convenience the molar ratio in the copolymer were further calculated and compared with the experimentally determined value through the relation (19).

$$F_1 = \frac{r_1 f_1^2 + f_1 f_2}{r_1 f_1^2 + 2 f_1 f_2 + r_2 f_2^2} \tag{1}$$

Table 3 illustrates the calculated and spectroscopic determination of molar ratios in the copolymer, reactivity ratios, and r_1r_2 product. The excellent agreement between experimental and calculated molar ratios of the formed copolymer emphasizes the exact determination of reactivity ratio values. Furthermore, the r_1r_2 product confirms, for both techniques, that the formed copolymer was of an alternating copolymer type.

3.6 Effect of Temperature on r_1r_2 Product

In our laboratory, we have investigated the exponential relationship between r_1r_2 product with temperature through Equation 2 as follows (20, 4):

$$r_1r_2 = \frac{A_{11}A_{22}}{A_{12}A_{21}} \exp\left(\frac{(E_{12}+E_{21})-(E_{11}+E_{22})}{RT}\right) \tag{2}$$

The overall activation energy [*i.e.* $\Delta E = (E_{12} + E_{21}) - (E_{11} + E_{22})$] can be determined from the plot of ($\boldsymbol{ln\,(r_1r_2)}$) with reciprocal of temperature ($\boldsymbol{1/T}$) as Equation 2 suggests, where E_{11} is the activation energy of monomer 1 to join M_1 macroradical chain and E_{22} is the activation energy of monomer 2 to join M_2 macroradical chain. Furthermore, E_{12} is the activation energy of monomer 2 to join M_1. macroradical chain and E_{21} is the activation energy of monomer 1 to join M_2. macroradical chain. Tables 4 illustrates a change of r_1r_2 product as temperature changes that were determined using the Kelen-Tudos technique.

Figure 7 shows the linear relationship of $ln\,(r_1r_2)$ vs. $1/T$, which was derived from Equation 2. The overall activation energy changes (*i.e.* $(E_{12} + E_{21}) - (E_{11} + E_{22})$) were found to be -118.4 kJ/mol. This value confirms the monomers prefer the alternating behavior (21) (*i.e.* M_1 prefers M_2 and M_2 prefers M_1) and consequently, the type of copolymer formed from MAAm and HEMA monomers would be analternating type, which is in accordance with values determined in Table 3.

Table 4. Change of r_1r_2 product as temperature changes

Temperature (°C)	r_1	r_2	r_1r_2
5	0.0334	0.0249	0.0008
10	0.0253	0.0252	0.0006
20	0.0875	0.2042	0.0179

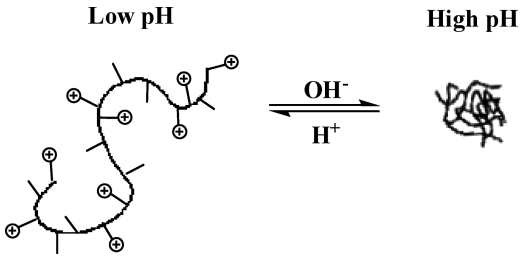

Sch. 1. Configurational change from open to globular agglomerate chain structure.

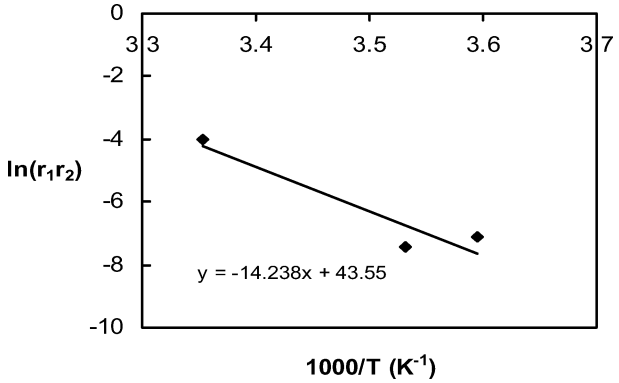

Fig. 7. Change of $\ln(r_1 r_2)$ vs. $1/T$.

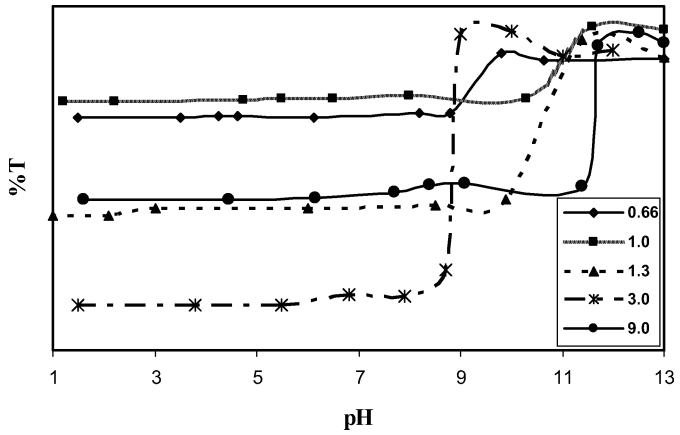

Fig. 8. Change in %Transmittance vs. pH.

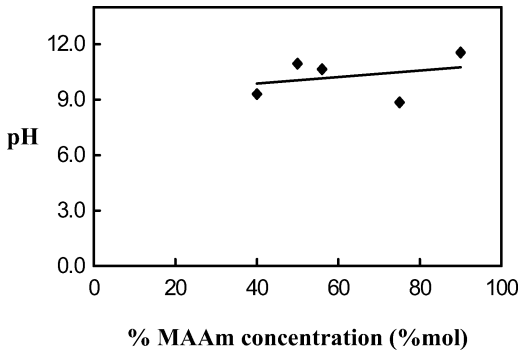

Fig. 9. Change of pH with MAAm monomer content (in mol%).

3.7 Phase Transition Determination

The reversible phase transition that sharply takes place upon exposing a smart pH-sensitive copolymer aqueous solution to increasing pH were studied by the cloud point technique using UV-Vis spectroscopy (21). This sharp transition from hydrophilic soluble state into a hydrophobic non-soluble state at certain pH, as seen in Figure 8, can be explained on the basis that in the soluble state, the polymer-solvent interactions are favored over polymer-polymer interactions, whereas in the non-soluble state, the polymer-polymer interactions are favored leading to precipitation (22). This configurational change from open chain structure to globular agglomerate chain structure, as depicted in Scheme 1, is mainly due to the presence charged atoms on the pendant groups.

These charged groups enhance polymer-solvent interactions, and on the other hand, prevent chain-chain interactions due to electrostatic repulsion between similar charged molecules, which cause an increase in polymer solubility in water solution. On the other hand, if such charged molecules are neutralized by pH change, the polymeric chain-chain interactions are then favored over polymer-solvent interactions which eventually lead to precipitation.

The introduction of neutral co-monomers, such as HEMA on MAAm in different fractions, had a large effect on the pH-sensitivity of the copolymers. Figures 8 and 9 illustrate the change of %transmittance versus pH, and change of pH as a function %MAAm concentration, respectively.

The sharp pH changes were observed for all the samples in Figure 8. Furthermore, these sharp transitions of pH values for the different molar feed ratios shown in Figure 9 confirm that linear relationship can be obtained between %MAAm and transient pH value. The obtained linearity starts with pH = 9.30 at 40 mol% MAAm (*i.e.* 60 mol% HEMA) and ends with pH = 11.55 at 90 mol% MAAm (*i.e.* 10% HEMA). These results emphasize that the HEMA content plays a crucial rule in the value of pH at which the copolymer could precipitate and disappears from the solution. Eventually; this change in pH values from 9.30 to 11.55 for the different molar ratios can be very helpful for choosing the pre-determined copolymer for drug release systems.

4 Conclusions

The smart pH-sensitive copolymers, prepared by different molar feed ratios of MAAm and HEMA, have yielded linear behavior in pH transition response, as Figure 8 suggests. The sudden transient pH value at 40 mol% MAAm (*i.e.* molar feed ratio = 0.66) have shown pH = 9.30, whereas at 90 mol% MAAm (*i.e.* molar feed ratio = 9.0) have shown transient pH = 11.55. This interesting feature could be very useful in choosing the type of copolymer

that can be de-accumulated at certain pH and conclusively releases the drug contained into it, and thus this class of copolymers can be successfully used in site specific release of drugs. Furthermore, the increasing molar feed ratios of such pH-sensitive copolymers have yielded a lowering in % crystallinity, a lowering in activation energies values, an increase in glass transition temperature (T_g) values, and conclusively a change in copolymer morphology from accumulated two-dimensional layers to flat slippery rigid amorphous structures. Finally, the types of the formed pH-sensitive copolymers, determined from Kelen-Tudos, Fineman-Ross techniques and from Equation 2, were found to be an alternating type with some random segments.

Acknowledgement

This work was financially supported and acknowledged by project number 43/2007, Jordan University of Science and Technology, Irbid, Jordan.

References

1. Zhou, G., He, J., Harruna, I. and Geckeler, K. (2008) *J. Mater. Chem.,* 18, 5492–5501
2. Berna, Y., Belma, I. and Mehmet, K. (2002) *Euro. Polym. J.*, 38, 1343–1447.
3. Grignon, J. and Scallan, A.M. (1980) *J. Appl. Polym. Sci*., 25, 2829–2843.
4. Fares, M.M. and Othman, A.A. (2008) *J. Appl. Polym. Sci*., 110 (5), 2815–2825.
5. Xu, F., Kang, E. and Neoh, K., (2006) *Biomaterials*, 27 (14), 2787–2797.
6. Liu, L., Fishman, M.L., Kost, J. and Hicks, K.B., (2003) *Biomaterials*, 24(19), 3333–3343.
7. Langer, R. and Peppas, N.A. (2003) Advances in Biomaterials, Drug Delivery, and Bionanotechnology, AIChE J., 49(12): 2990–3006.
8. Zhang, X.Z., Wu, D.Q. and Chu, C.C. (2004) *Biomaterials*, 25(17), 3793–3805.
9. Jeong, B. and Gutowska, A. (2002) *Trends in Biotechnology*, 20(7), 305–311.
10. Qiu, Y. and Park, K. (2001) *Adv. Drug Deliv. Rev*., 53(3), 321–339.
11. Zhang, X.Z., Yang, Y.Y., Chung, T.S. and Ma, K.X. (2001) *Langmuir*, 17(20), 6094–6099.
12. Zhang, W., Shi, L., Wu, K. and An, Y. (2005) *Macromolecules*, 38, 5743–5747.
13. Rihova, B., Bilej, M., Vetvicka, V., Ulbrich, K., Strolahm, J. and Duncan, R. (1989) *Biomaterials*, 10, 335–342.
14. Kelen, T. and Tudos, J. (1975) *Macromol. Sci. Chem. Ed*., 9, 1–9.
15. Fineman, M. and Ross, S.D. (1950) *J. Polym. Sci*., 5(1): 259–262.
16. Carraher, C.E. Polymer Chemistry, 6th Ed. Marcel-Dekker: New York, 83–87, 2003.
17. Hulubei, C. and Morariu, S. (2000) *High Perform. Polym*., 12(4), 525–533.
18. Alfrey, T.J. and Price, C.C. (1947) *J. Polym. Sci*., 2, 101.
19. Odian, G. Principles of Polymerization, 4th Ed. Wiley-Interscience: New York, 506–510, 2004.
20. Fares, M.M. (2008) *Open Macromol. J*., 2, 1–5.
21. Eeckman, F., Amighi, K. and Moes, A.J. (2001) *Int. J. Pharm*., 222(1), 259–270.
22. Loh, W. and Da Silva, R.C. (1998) *J. Coll Interface Sci*., 202(1), 385–390.